inter.noise 2014
MELBOURNE AUSTRALIA
16-19 NOVEMBER

Active reduction of sound transmission in aircraft cabins: a smarter use of vibration exciters

Romain BOULANDET[1]; Marc MICHAU[2]; Philippe MICHEAU[3]; Alain BERRY[4]

[1,2,3,4] Groupe d'Acoustique de l'Université de Sherbrooke (GAUS), J1K 2R1, Sherbrooke, Québec, Canada
[2] Laboratoire de Mécanique et d'Acoustique, CNRS, UPR7051, Aix-Marseille Univ., Centrale Marseille, France

ABSTRACT

This paper addresses an active structural acoustic control (ASAC) approach to reduce sound transmission through an aircraft trim panel. The focus is on the practical implementation of the virtual mechanical impedance approach through self-sensing actuation instead of using sensor-actuator pairs. The experimental setup includes two sensoriactuators designed from an electrodynamic inertial exciter and distributed over an aircraft trim panel, which is subject to a time-harmonic diffuse sound field. A methodology based on the experimental identification of key parameters of the actuator is proposed, wherein the vibration of the structure is estimated from the electrical signals picked up at the input terminals of the transducer. Measured data are compared to results obtained with conventional sensor-actuator pairs consisting of an accelerometer and an inertial exciter, particularly as regards sound power reduction. The decrease of sound power radiated is comparable in both cases and equals 3 dB when the panel is controlled at the excitation frequency of 363 Hz, as expected by optimal calculation for two control units.

Keywords: ASAC, Transmission, Sensoriactuators I-INCE Classification of Subjects Number(s): 38.3

1. INTRODUCTION

In recent decades, there has been a growing interest in composite materials in the aircraft industry because they allow the structural weight of the aircraft to be decreased, and hence a reduced fuel consumption. However, the combination of high stiffness and low mass is unfavorable in terms of radiated noise, increasing the sound transmission efficiency of the cabine against outside noise. The use of sound absorbing materials to improve sound insulation is widely studied, but still penalized by added mass and a poor efficiency at low frequencies. Many active methods, including active structural acoustic control (ASAC) strategies, have been developed to reduce sound radiation and transmission through panel-like structures (1, 2, 3). When flexural structures made up of a large number of resonant modes and a low structural damping are considered, active damping is most often the best option since the reduction in the amplitude of the resonance peaks causes a decrease in the radiated sound power (4, 5, 6). In the case of flexural structures with a high inherent structural damping like the composite panels commonly used in aircraft cabins, it has been shown that the active damping approach does not allow the noise transmitted to be reduced effectively (7).

Unlike the active damping approach, wherein the feedback gain is real positive and provides an additional viscous damping, the implementation of active mechanical impedances may be necessary to optimally minimize the radiated sound power. As first shown experimentally by Guicking *et al.* (9), structural vibrations can be controlled effectively, provided that the mechanical input impedances can be set to target values, spanning a wide range of a real part and imaginary part. On the footsteps of (9), other methods based on impedance control have been developed for aircraft applications (10), including the virtual mechanical impedance approach (11). This concept is basically to impose, at a given frequency, a linear complex-valued relationship between two variables, most often from a colocated sensor-actuator pair attached to the structure. When the variables are dual, moreover, their product is proportional to the power supplied to the structure and the desired mechanical impedances are applied directly. In practice, however, sensor-actuator pairs can hardly be collocated and conditions ensuring duality are not always respected in the whole frequency range (12).

[1] romain.boulandet@usherbrooke.ca
[2] marc.michau@usherbrooke.ca
[3] philippe.micheau@usherbrooke.ca
[4] alain.berry@usherbrooke.ca

In this paper, we discuss the practical implementation of the virtual mechanical impedance concept using electrodynamic sensoriactuators (13). The remaining is organized as follow. In Section 2, it is shown how an electrically-actuated inertial exciter can be readily turned into a sensoriactuator. The baseline concept of the virtual mechanical impedance is presented in Section 3, along with its practical implementation using a complex envelope controller (14). Experimental results performed on an aircraft trim panel using sound transmission loss facilities are provided in Section 4. Finally, findings and conclusions highlight the benefits of using an electrodynamic actuator to perform self-sensing actuation, and thus locally control the mechanical impedance of structures without the need for external sensors.

2. ELECTRODYNAMIC INERTIAL EXCITER

2.1 Governing equations

An electrodynamic inertial exciter is a reversible voice coil transducer which has capability to provide input vibrational energy to a host mechanical structure. As illustrated in Fig. 1, it can be regarded as a two-port system, including an electromechanical coupling through two pairs of dual variables: the voltage e and current i for the electrical side, and the transverse force F_s and velocity v_s for the mechanical side.

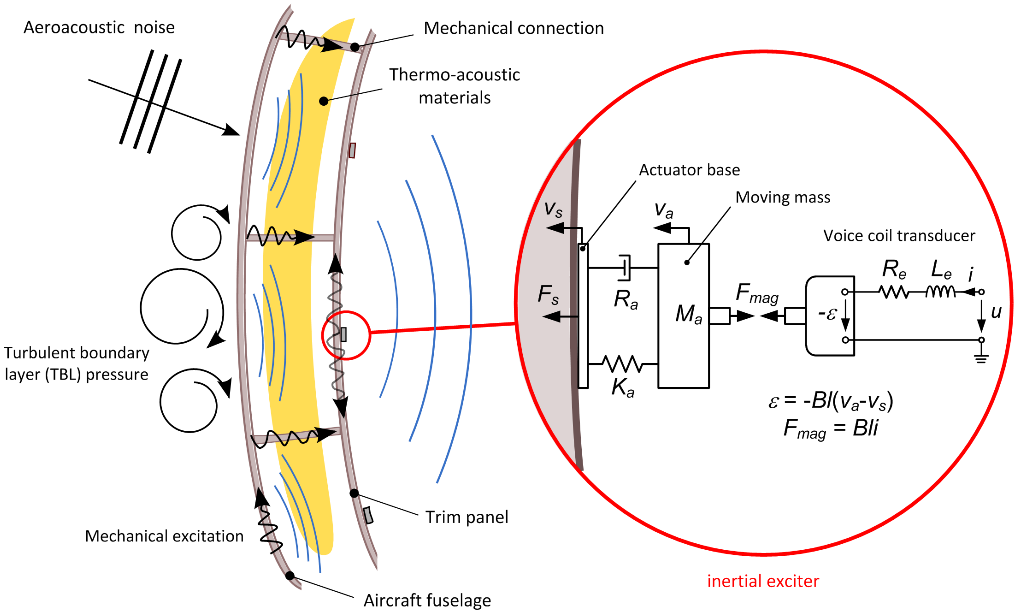

Figure 1 – Schematic representation of the electrodynamic inertial exciter when coupled to the aircraft trim panel.

Using phasors to represent the complex amplitude (magnitude and phase) of sinusoidal functions of time, the characteristic equations of the inertial exciter when attached to a host mechanical structure can be written as (13, 15)

$$Bl\,\underline{i} = \underline{Z}_{ma}\,\underline{v}_a - \underline{Z}_{ms}\,\underline{v}_s \quad (1)$$

$$\underline{e} = \underline{Z}_e\,\underline{i} - \underline{\varepsilon} \quad (2)$$

where $\underline{v}_a$ is the velocity of the moving mass, $\underline{v}_s$ is the transverse velocity at the base of the actuator, $\underline{e}$ is the input voltage applied to the electrical terminals, $\underline{i}$ is the current circulating in the coil, $\underline{Z}_{ma} = j\omega M_a + R_a + K_a/j\omega$ is the mechanical impedance of the inertial exciter, $\underline{Z}_e = R_e + j\omega L_e$ is the blocked electrical impedance of the transducer, and $\underline{Z}_{ms} = R_a + K_a/j\omega$ is the impedance of the spring-dashpot mounting system. Equations (1-2) contain terms of electrodynamic coupling ; $\underline{F}_{mag} = Bl\,\underline{i}$ is the force caused by the interaction of the magnetic field and the moving free charges (current), and $\underline{\varepsilon} = -Bl(\underline{v}_a - \underline{v}_s)$ is the back electromotive force (voltage) induced within the voice coil during motion. It is also assumed that all the forces acting on the actuator are small enough so that the displacements remain proportional to applied forces (small-signal assumptions). The physical parameters of the inertial exciters used in this study can be found in Table 1.

Table 1 – Physical parameters of the electrodynamic inertial exciter measured in small-signal range.

Parameter	Notation	Value	Unit
dc resistance	R_e	3.36	Ω
Voice coil inductance	L_e	0.05	mH
Transduction coefficient	Bl	4.4	$\mathrm{N\,A^{-1}}$
Moving mass	M_a	0.125	kg
Mechanical resistance	R_a	0.31	$\mathrm{N\,m^{-1}\,s}$
Suspension stiffness	K_a	$17.5\,10^3$	$\mathrm{N\,m^{-1}}$
Natural frequency	f_n	59.6	Hz

2.2 Input impedance

The input impedance of the inertial exciter is the complex ratio of the voltage to the current in the electrical circuit of the transducer. It determines the electrical impedance (in Ω) 'seen' by any equipment such as electronic drive source, electrical network, etc., connected across its input terminals. When attached to a pure mass, the closed form expression of the input impedance of the inertial exciter can be obtained by combining Eq. (1) and (2), as

$$\underline{Z}_{in} = \frac{\underline{e}}{\underline{i}} = \underline{Z}_e + \frac{(Bl)^2}{\underline{Z}_{ma}} \tag{3}$$

As can be seen in Eq. (3), $\underline{Z}_{in}$ contains all the electromechanical effects that are operating, including all resistances and reactances of the actuator impedance. As discussed in the following, measuring the input impedance of the actuator enables certain key parameters such as the dc resistance and natural frequency to be evaluated.

2.3 Self-sensing actuation

Substituting now Eq. (1) in Eq. (2), the transverse velocity at the base of the actuator be expressed as (13)

$$\underline{v}_s = -\frac{\underline{Z}_{ma}}{j\omega M_a Bl}\left(\underline{e} - \underline{Z}_e\,\underline{i}\right) + \frac{Bl}{j\omega M_a}\,\underline{i} \tag{4}$$

Equation (4) clearly shows that the transverse velocity of the structure where the actuator is located can be estimated from the driving current and the voltage sensed at its input terminals. In addition, for frequencies such that $\sqrt{K_a/M_a} < \omega < R_e/L_e$, i.e. above the natural resonance of the inertial exciter and below the cut-off frequency of the coil electrical filter, a simplified expression of Eq. (4) can be obtained as

$$\underline{v}_s \simeq -\frac{\underline{e}}{Bl} + \left(\frac{R_e}{Bl} - j\frac{Bl}{\omega M_a}\right)\underline{i} \tag{5}$$

As shown in Eq. (5), three physical parameters of the transducer, namely the electrodynamic transduction coefficient Bl, the moving mass M_a, and the dc resistance R_e, are needed to turn the inertial exciter into a sensoriactuator.

3. ACTIVE IMPEDANCE CONTROL STRATEGY

3.1 Virtual mechanical impedance concept

The concept of virtual mechanical impedance is to simply impose a linear complex-valued relationship between dual and collocated variables, which are strategically located on the structure so that vibration can be effectively sensed and controlled (11). Assuming a linear, time-invariant (LTI) system and without considering the coupling between the electromechanical transducers and the structure, the system to be controlled can be expressed in matrix form (15), as

$$\mathbf{v}_s = \mathbf{Y}\,\mathbf{f}_s + \mathbf{d} \tag{6}$$

where $\mathbf{v}_s$ is the vector of structural velocity (in $\mathrm{m\,s^{-1}}$), typically the output signals of the velocity sensors, $\mathbf{f}_s$ is the vector of the force applied (in N), typically the point force input signals, $\mathbf{Y}$ is the matrix of the mobility functions of the structure (in $\mathrm{m\,s^{-1}\,N^{-1}}$) at the control points, and $\mathbf{d}$ is a vector that takes into account the primary acoustic excitation at the sensors location.

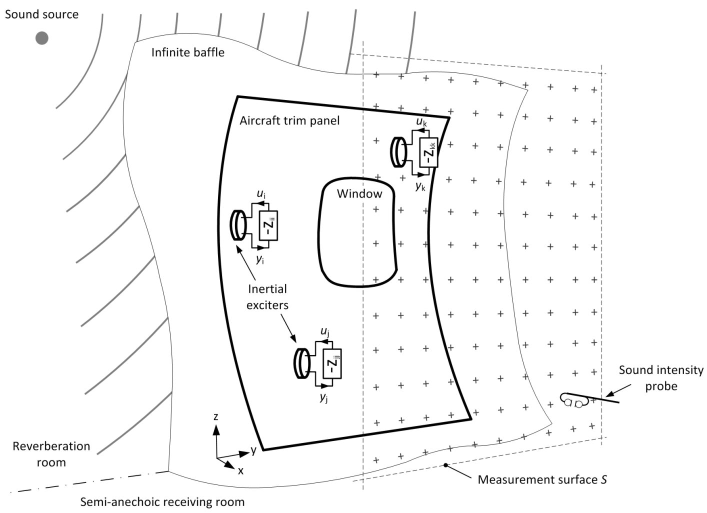

Figure 2 – Schematic representation of the virtual mechanical impedance principle applied to an aircraft panel.

The control objective is to determine the optimal mechanical impedances $\mathbf{Z}_m$ to be applied between the dual variables $\mathbf{f}_s$ and $\mathbf{v}_s$ that effectively reduces the radiated sound power, which can be written mathematically as

$$\mathbf{f}_s = -\mathbf{Z}_m \mathbf{v}_s \tag{7}$$

where $\mathbf{Z}_m$ is a diagonal matrix which connects the input force and the velocity response of the structure at the control points. It is worth mentioning that combining Eqs. (6) and (7) leads to implement a feedback control system that is unconditionally stable, provided the compensator is positive real, i.e. $\mathrm{Re}\left[\mathbf{Z}_m\right] > 0$ for any angular frequency ω (4).

3.2 Linear quadratic control

The calculation of the optimal mechanical impedances is done by solving a linear quadratic optimal control problem. As the control objective is the minimization of sound power radiated, the quadratic cost functional is expressed in terms of the active sound intensity as

$$J = \frac{S}{2N_S}\mathrm{Re}\left[\mathbf{v}^H\mathbf{p}\right] \tag{8}$$

where $\mathbf{p}$ and $\mathbf{v}$ are the vectors of complex amplitudes of the sound pressure and particle velocity on the surface S, respectively, and N_S is the number of measurement points. Both the sound pressure and particle velocity can then be expressed as a function of the control inputs $\mathbf{u}$ (current or voltage) applied to the actuators using linear transfer functions, and the optimal control inputs $\mathbf{u}^{opt}$ can be derived by solving $\nabla_{\mathbf{u}}J = 0$. More details on the calculation of the optimal control inputs can be found in (8).

Last, the elements of the diagonal complex-valued matrix $\mathbf{Z}$ to be imposed between the control inputs $\mathbf{u}$ and output signals $\mathbf{y}$ as illustrated in Fig. 2 can be written as

$$\underline{Z}_{ii} = -\frac{\underline{u}_i^{opt}}{\underline{y}_i^{opt}} \qquad \text{where} \qquad \mathbf{y}^{opt} = \mathbf{H}\,\mathbf{u}^{opt} + \mathbf{d} \tag{9}$$

where $\mathbf{H}$ is the matrix of the transfer functions between the sensors and actuators. As can be seen in Eq. (9), an optimal virtual impedance can be defined for each control unit and the effective mechanical impedance applied to the structure as given in Eq. (7) can be expressed in terms of $\mathbf{Z}$, provided the actuator efficiency and sensor sensitivity are known.

3.3 Complex envelope controller

In some cases the optimal virtual impedances $\mathbf{Z}$ determined by calculation may be negative real part and a practical way to implement is to use a real-time complex envelope controller (14), the function of which can be expressed as

$$\frac{d\mathbf{u}}{dt} = -\mu\mathbf{C}\left[\mathbf{u} + \mathbf{Z}\,\mathbf{y}\right] \tag{10}$$

where μ is a gain coefficient and $\mathbf{C}$ is a complex-valued compensation matrix. In order to ensure the stability of the algorithm (10), $\mathbf{C}$ needs to be considered so that $\mathrm{Re}\left[\lambda_i\left\{\mathbf{C}\left(\mathbf{I}+\mathbf{Z}\,\mathbf{H}\right)\right\}\right] > 0\ \forall i = 1\cdots N_a$ with N_a the number of actuators, where $\lambda_i\{\cdot\}$ denotes the i-th eigenvalue of $\{\cdot\}$. Note that in the case of centralized control $\mathbf{C}$ is fully populated while it is diagonal in decentralized control. More details about the tuning of the compensation matrix $\mathbf{C}$ can be found in (7).

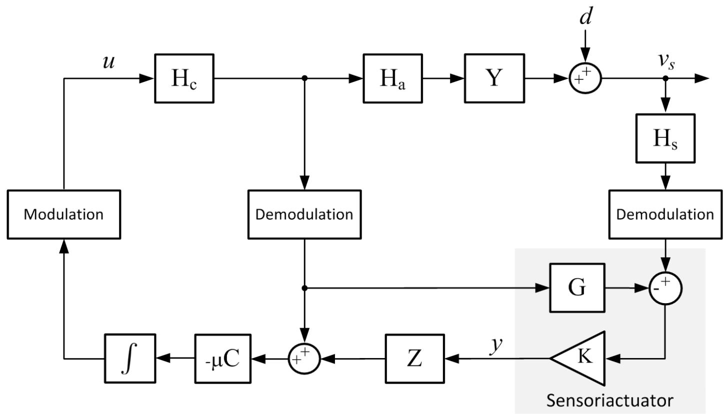

Figure 3 – Block diagram of the control scheme for a single sensoriactuator.

Figure 3 illustrates the basic control scheme for a single sensoriactuator. As shown in Fig. 3, the controlled variable y depends on the output signal $H_s v_s$ sensed at the terminals of the actuator and the control signal $H_c u$ used for actuation, where H_s is the transfer function between the transverse velocity at the control point and the voltage delivered at the terminals of the actuator and H_c is the transfer function of the electronic circuit used to drive the actuator. In this study, the control signal is the current i in Eq. (1) that drives the actuator and the output signal is the voltage generated at the input terminals of the actuator. The complex-valued matrix $G(\omega) = R_e - j(Bl)^2/\omega M_a$ and the gain matrix $K = 1/Bl$ shown in Fig. 3 are needed to obtain the transverse velocity estimate v_s, in accordance with Eq. (5). Note that in the case of a conventional sensor-actuator pair, the controlled variable y is directly the output signal of the accelerometer after processing by a time integrator.

4. RESULTS

4.1 Determination of the linear parameters of the actuator

Unlike the self-sensing approach developed in (16) using various types of electrical network connected to a shaker, a model-based approach is proposed here to achieve self-sensing actuation. As previously mentioned, the estimation of the linear parameters needed for self-sensing actuation is based on the measurement of the electrical impedance. In practice, this is done by measuring the electrical signals at the transducer terminals in the small signal domain where nonlinear distortion in voltage and current can be neglected. In this study, we used a swept sinusoidal excitation in the frequency range 10 Hz – 2 kHz.

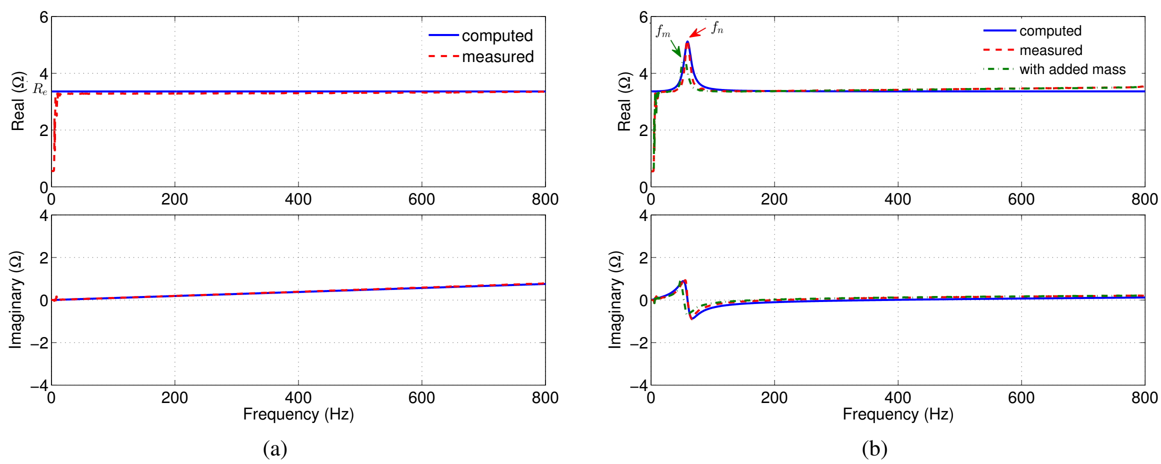

Figure 4 – Computed and measured blocked electrical impedance of the voice coil (a) and input impedance of the inertial exciter when attached to a pure mass (b).

Figure 4 shows the frequency response function of the blocked electrical impedance (a) and the electrical input impedance of the inertial exciter when attached to a pure mass (b). The dc resistance R_e of the voice coil is obtained from the blocked electrical impedance $\underline{Z}_e$ in Eq. (2), i.e. by clamping the voice coil within the magnet assembly to remove the motional part of the impedance. As can be seen in Fig. 4(a), R_e is the value when the frequency response function approaches zero. The dynamic mass M_a of the inertial exciter is estimated by measuring the input impedance of the actuator when coupled to a pure mass. This allows the motional impedance in Eq. (2) to be considered in the measurement of the input impedance, as shown in Fig. 4(b). One technique commonly employed requires a second (perturbed) measurement where an added mass m is attached to the moving parts of the actuator. Denoting f_m and f_n the two natural frequencies (in Hz) with and without added mass, respectively, the dynamic mass M_a can then be derived after

$$M_a = \frac{{f_m}^2}{{f_n}^2 - {f_m}^2} m \tag{11}$$

With an added mass $m = 0.033$ kg, the measured natural frequency of the actuator $f_n = 59.6$ Hz is found to be shifted at $f_m = 53$ Hz, thus determining the dynamic mass $M_a = 0.125$ kg. Note that for the transduction coefficient Bl, we used the value provided by the manufacturer. The values of the physical parameters measured in small-signal range can be found in Table 1.

As can be seen in Fig. 4, there is a good agreement between the measured and computed electrical input impedances. Measuring the input impedance of the actuator when coupled to a pure mass is therefore helpful to obtain the physical parameters of the vibration exciter which are required for the self-sensing actuation.

4.2 Experimental setup

This section presents experimental results performed on an aircraft composite panel comprising a window. Measured data were obtained using the sound transmission loss test facility depicted in Fig. 5. As can be seen in Fig. 5(a), a sound intensity probe is used both to determine the transfer functions necessary to calculate the optimal input impedances to be imposed to the structure, and to evaluate the acoustic power radiated by the panel in the receiving room, as given in Eq. (8). Sound intensity was measured on a grid of 7×7 points using an automated robot, as shown also in Fig. 5(a). The test panel was subject to a diffuse sound field that is generated by a sound source located in the reverberation room, as shown in Fig. 5(b). In this study, two

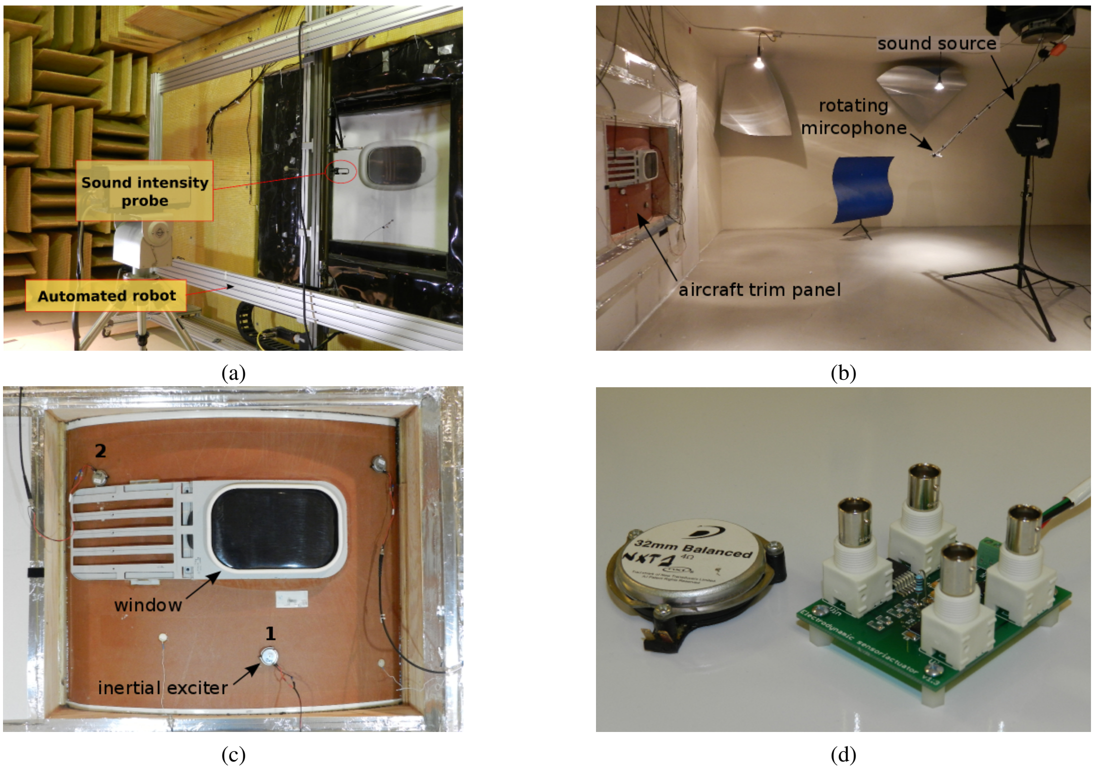

Figure 5 – Experimental setup using sound transmission loss facility: automated measurement of sound intensity in a semi anechoic room (a), location of the sound source in the reverberation room (b), arrangement of the two actuators on the aircraft trim panel (c), and picture of the inertial exciter and electronic drive circuit.

inertial exciters used as control units were fixed on the panel (source side) with a thin layer of adhesive glue, as illustrated in Fig. 5(c). A more detailed view of the inertial actuator model and the electronic circuit used both for actuating and sensing the electrical quantities at the transducer terminals is shown in Fig. 5(d). The digital signal processing needed to run the controller is performed using a Speedgoat Performance Real-Time Target Machine running on Simulink® Real-Time. Signal acquisition was done with 18 bit precision analog inputs at a sampling frequency of 20 kHz. As discussed in Section 3, an experimental identification of the relationships between all the noise and vibration sources and the total sound power radiated on the measurement surface is necessary. This includes determining the transfer functions between the primary sound source, the control inputs and the sound intensity probe, and also the transfer functions between actuators and sensors.

4.3 Control performance

The following section shows results obtained on the composite aircraft panel when it is subject to a diffuse sound field generated by a loudspeaker at the excitation frequency of 363 Hz, for a sound pressure level equal to 96.7 dB. The main focus of the analysis is on the comparison of the two ways to implement the method of virtual mechanical impedances, i.e. using sensor-actuator pairs compared with sensoriactuators.

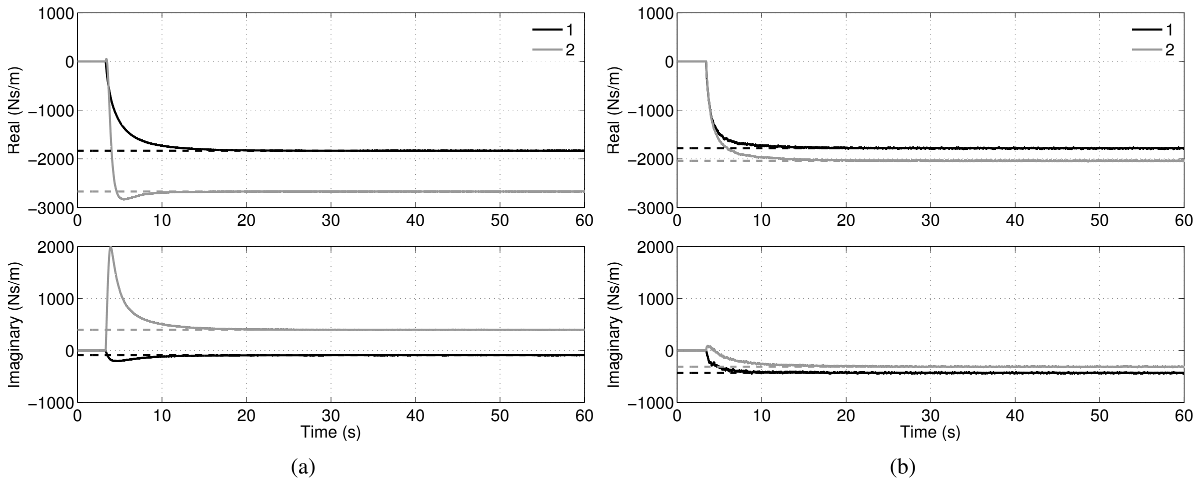

Figure 6 – Measured time data (solid line) to reach the target virtual impedance (dashed line) for the two sensor-actuator units (a) and for the two sensoriactuators (b).

As illustrated in Fig. 6, the input mechanical impedances imposed to the panel by the controller reach the target values perfectly, both the real part and the imaginary part. This applies for both the sensor-actuator pairs and the sensoriactuators. However, target values achieved in both cases are slightly different, probably due to a change in the primary acoustic field generated in the reverberation chamber and the modification of transfer functions previously determined which ensues. This has no effect on the overall performance of the panel under control since the resulting radiated sound power is comparable. As shown in Fig. 7, a decrease of 3 dB of sound power transmitted is obtained in both cases and the measured sound intensity maps are very similar when the panel is under control. Table 2 summarizes the virtual mechanical impedances that are imposed to the panel, which were calculated by optimal control as given in Eqs. (8-9), and the corresponding sound power reduction. Note that measured data were obtained using a decentralized controller.

Table 2 – Measured performance with no control and optimal virtual impedance control at the excitation frequency of 363 Hz.

Case		**Virtual mechanical impedance** ($\mathrm{N\,s\,m^{-1}}$)	**Radiated sound power** (re. 10^{-12}W)
no control			69.6 dB
sensor-actuator	# 1	$\underline{Z}_{11} = -1830 - 90j$	66.5 dB
	# 2	$\underline{Z}_{22} = -2670 + 400j$	
sensoriactuator	# 1	$\underline{Z}_{11} = -1780 - 430j$	66.3 dB
	# 2	$\underline{Z}_{22} = -2040 - 310j$	

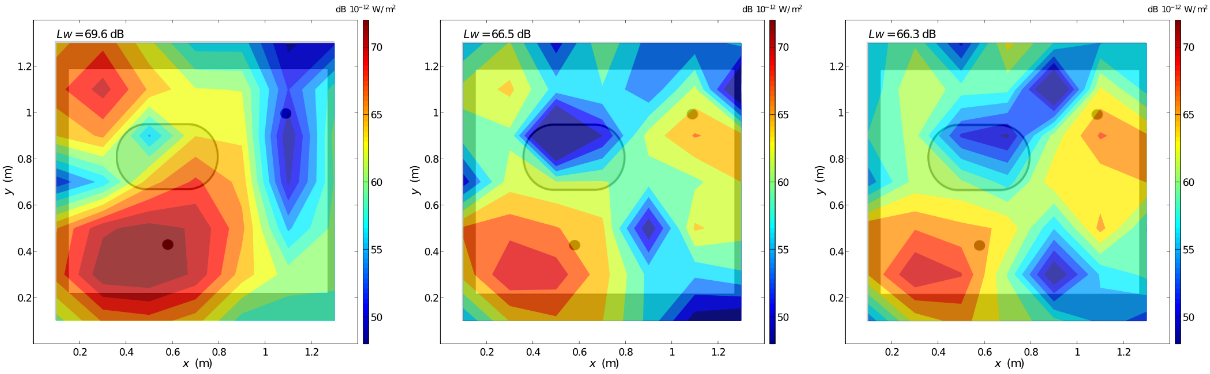

(a) (b) (c)

Figure 7 – Sound intensity map measured with no control (a) and with virtual mechanical impedance control using sensor-actuator units (b) and sensoriactuators (c).

4.4 Discussion

The development of sensoriactuator as detailed in Section 2 is equally effective for implementing the virtual mechanical impedances method in practice. It is clear from this study that the voice coil actuator is well suited to be used as a sensoriactuator for active structural acoustic control, especially for the following reasons:

- the transverse force which is transmitted to the structure by the actuator is directly proportional to input current through the electrodynamic coupling coefficient,
- the transverse velocity of the structure at the control point can be easily estimated from the electrical signals sensed at the terminals of the actuator, provided that some physical parameters of the actuator are known,
- the control input and controlled variable are clearly dual and collocated, thereby maintaining the passivity of the system.

This makes the inertial exciter particularly interesting in comparison to other competing technologies such as piezoceramics for example (13). In particular, the transfer function between the control and observation signal is proportional to the mobility of the structure, thereby making easier the physical interpretation of the effect of control over the structure.

It is also shown that in the case of the studied composite panel, i.e. a flexural structure with a high inherent structural damping, the virtual mechanical impedance method stands out from the active damping approach. Unlike the latter case wherein $\mathbf{Z}_m \in \mathbb{R}^+$, the target mechanical impedances derived by optimal control in order to reduce the radiated sound power are found to be complex numbers with negative real part, as shown in Table 2.

5. CONCLUSIONS

In this paper, the virtual mechanical impedance approach is implemented using sensoriactuators to achieve active reduction of sound transmission through an aircraft trim panel. It is shown that a conventional electrodynamic inertial exciter can be readily used for self-sensing actuation, while ensuring dual and collocated variables. A model-based methodology is proposed, wherein the vibration of the structure is estimated from the electrical signals picked up at the terminals of the transducer. It is also explained how to experimentally determine the key parameters of the inertial actuator that are required to turn it into a sensoriactuator. Measured data are compared to results obtained with conventional sensor-actuator pairs consisting of an accelerometer and an inertial exciter. Although the target mechanical impedances that result from the optimal calculation differ slightly, the decrease of sound power radiated is comparable in both cases and equals, as expected by calculation for two control units, 3 dB when the panel is controlled at the excitation frequency of 363 Hz.

ACKNOWLEDGEMENTS

This work was supported by the Swiss National Science Foundation (SNSF), the National Sciences and Engineering Research of Canada (NSERC) and Bombardier Aerospace.

REFERENCES

1. C. R. Fuller, S. J. Elliott and P. A. Nelson, *Active control of vibration*, Academic Press Inc., 1996
2. S. J. Elliott and M. E. Johnson, *Radiation modes and the active control of sound power*, J. Acous. Soc. Am., *94*, pp 2194-2204, 1993
3. J. P. Maillard and C. R. Fuller, *Advanced time domain wave-number sensing for structural acoustic system - I. Theory and design*, J. Acous. Soc. Am., **95**(6), pp 3252-3261,1994
4. S. J. Elliott, P. Gardonio, T. Sors and M. J. Brennan, *Active vibroacoustic control with multiple local feedback loops*, J. Acous. Soc. Am., **111**, pp 1487-1495, 2002
5. Ch. Paulitsch, P. Gardonio and S. J. Elliott, *Active vibration control using an inertial actuator with internal damping*, J. Acoust. Soc. Am., **119**(4), 2006
6. P. Gardonio, S. Miani S., F. Blanchini, D. Casagrande and S. J. Elliott, *Plate with decentralised velocity feedback loops: Power absorption and kinetic energy considerations*, J. Sound. Vib., **331**, pp 1722-1741, 2012
7. P. Micheau, M. Michau, R. Boulandet, A. Berry and P. Herzog, *Decentralized Complex Envelope Controller for ASAC by Virtual Mechanical Impedances*, Proceedings IEEE/ASME International Conference on Advanced Intelligent Mechatronics, Besançon, France, 2014
8. M. Michau, A. Berry and P. Micheau, *Optimal virtual mechanical impedances approach for the vibroacoustic active control of a panel*, In proceedings of the 21st International Congress on Sound and Vibration, Beijing, China, 2014
9. D. Guicking, J. Melcher and R. Wimmel, *Active impedance control in mechanical structures*, Acta Acustica united with Acustica, **69**(2), 1989
10. P. J. Remington, A. R. D. Curtis, R. B. Coleman and J. Scott Knight, *Reduction of turbulent boundary layer induced interior noise through active impedance control*, J. Acoust. Soc. Am., **123**(3), 2008
11. N. Quaegebeur, P. Micheau, and A. Berry, *Decentralized harmonic control of sound radiation and transmission by a plate using a virtual impedance approach*, J. Acous. Soc. Am., **125**(5), 2009
12. Q. Sun, *Some observations on physical duality and collocation of structural control sensors and actuators*, J. Sound. Vib., **194**, pp 765-770, 1996
13. R. Boulandet, A. Pelletier, P. Micheau and A. Berry, *Active vibration control using self-sensing actuators : an experimental comparison of piezoelectric and electromagnetic technologies*, In proceedings of the ASME Inter. Mech. Eng. Congress & Exposition, Montréal, Canada, 2014
14. P. Micheau and S. Renault, *Active control of the complex envelope associated with a low damped mode*, Mech. Syst. and Signal Proc., **20**(3), 2006
15. F. Fahy and P. Gardonio, *Sound and structural vibration : Radiation, transmission and response*, Elesevier Academic Press, 2007
16. C. Paulitsch, P. Gardonio and S. J. Elliott, *Active vibration damping using self-sensing, electrodynamic actuators*, Smart Mater. Struct., **15**, pp 499-508, 2006